Heat transfer mediated by the dynamical Casimir effect in an optomechanical system

Lei-Lei Nian and Jing-Tao Lü *

School of Physics and Wuhan National High Magnetic Field Center,
Huazhong University of Science and Technology, Wuhan 430074, People's Republic of China

(Received 11 March 2021; revised 13 May 2021; accepted 1 June 2021; published 21 June 2021)

Heat transfer in an optomechanical system consisting of one optical cavity and two movable mirrors with or without a laser field is studied by using the quantum master-equation method. The radiation-pressure interaction between the cavity and the mirrors contains the single-photon optomechanical coupling (SPOC) and the dynamical Casimir effect (DCE). When the laser is not applied to the cavity, the heat transfer is induced by a nonlocal interaction between mirrors that builds up only due to the presence of the DCE. Once the monochromatic field is turned on, both the SPOC and the DCE can be used to modify the energy transfer process. In both cases, the heat transfer can be drastically enhanced at resonant conditions manifested by the DCE. Our results can motivate further studies to actively control heat transfer mediated by the DCE in optomechanical devices.

DOI: 10.1103/PhysRevA.103.063510

I. INTRODUCTION

In optomechanical systems, the electromagnetic cavity mode and vibrations of mechanical resonators couple to each other via radiation pressure force [1–4]. The resulting optomechanical coupling, as an important type of light-matter interaction, plays a key role in engineering quantum states of the cavity and the mechanical modes. In weakly driven optomechanical systems, a conventional photon blockade due to the presence of single-photon strong coupling can be obtained [5,6]. In the weak optomechanical-coupling regime, an unconventional photon blockade induced by destructive quantum interference between different excitation pathways for a two-photon state can also be observed [7,8]. Moreover, the resonant frequency of the mechanical resonators and their damping can be mediated indirectly by the optomechanical coupling; then the mechanical resonators can be cooled to their ground state, where the quantum limited measurements and observations become possible [9–16]. Furthermore, it is possible to prepare the mechanical resonators in nonclassical states using the optomechanical interaction [17,18].

On the other hand, when the optomechanical systems contain two movable mirrors in an optical cavity, the radiation-pressure interaction can give rise to a nonlocal coupling between the mechanical modes, such that the energy and the quantum states can be exchanged between them [19–26]. Based on this, heat transfer induced by quantum fluctuations was observed in experiment recently [27]. The quantum fluctuations indicate the quantum vacuum is not empty, in which virtual particles can be transformed into real ones by the Schwinger process [28], Hawking radiation [29], and Unruh effect [30]. The dynamical Casimir effect (DCE) proposed by Moore in 1970 is a very intuitive embodiment of the interesting prediction from quantum field theory [31] which states that the creation of photons from the quantum vacuum can be achieved by constructing a time-dependent boundary condition. In cavity-optomechanical systems, the DCE takes place when one or both of the mirrors is subjected to nonuniform acceleration [22,32–37]. For instance, once the two mirrors are positioned near two thermal baths with different temperatures, heat transfer induced by the DCE can be observed [27]. Thus, one can detect the virtual particles in quantum vacuum and their conversion into phonons by measuring the thermodynamic quantities, such as heat flux. Normally, the DCE will be significantly weakened when the cavity frequency is far from the mechanical frequencies supported by the mirrors, while the single-photon optomechanical coupling (SPOC) can yield a heat transfer when the cavity is driven by coherent light [24,38–42]. These substantial developments open a way to generate and regulate the quantum heat transfer mediated by the DCE and the SPOC, although it is unknown which plays the leading role, especially when the cavity frequency and the mechanical frequencies are comparable. Meanwhile, the near-field thermal radiation is a normal process in such optomechanical devices, which may accompany or influence the heat transfer. Therefore, to observe the DCE-induced heat transfer, it is necessary to study how to highlight the role of the DCE in such an energy transfer processes.

In this paper, we study the heat transfer of an optomechanical system consisting of one optical cavity and two movable mirrors, which is driven by a temperature bias, as shown in Fig. 1. The radiation-pressure interaction between the cavity and the mirrors contains the SPOC and the DCE. We first examine the DCE contributions to the heat transfer when the cavity is not excited by a laser. It is found that a nonlocal energy transfer between mirrors is induced only by the DCE, which is consistent with the experimental observations [27]. For a laser-driven cavity, we remark that it is possible to generate the nonlocal energy transfer by both the SPOC and the DCE, where the former has been observed [42]. Importantly, the resonance-enhanced energy transfer can be

*jtlu@hust.edu.cn

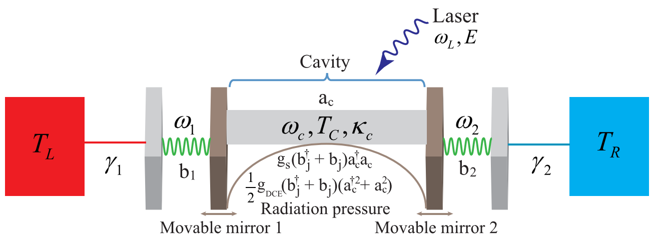

FIG. 1. Setup for the heat transfer in an optomechanical system consisting of one cavity and two mechanically moving mirrors. The cavity mode (a_c) with frequency ω_c is coupled to the mechanical modes (b_1 and b_2) with frequencies ω_1 and ω_2 via the radiation pressure. The radiation pressure drives the SPOC and the DCE, which are marked by g_s and $g_{\rm DCE}$. The cavity and mechanical oscillators are coupled to external baths with coupling strengths γ_1, γ_2, and κ_c. Assuming that the baths are in thermal equilibrium with temperatures T_L, T_R, and T_C. The cavity is driven by an external weak laser field with frequency ω_L and amplitude E.

obtained, which yields a way to highlight the DCE's role in the heat transfer.

II. MODEL AND METHOD

The optomechanical system in Fig. 1 is composed of a cavity and two mechanical resonators; their interaction is via the radiation pressure. The cavity and the two mechanical oscillators are coupled to the thermal baths. The model Hamiltonian is

$$H = H_s + H_b + H_{s-b}, \tag{1}$$

where H_s describes the optomechanical system ($\hbar = 1$)

$$\begin{aligned} H_s = {} & \omega_c a_c^\dagger a_c + \sum_{j=1,2} \omega_j b_j^\dagger b_j + E a_c^\dagger e^{-i\omega_L t} + E^* a_c e^{i\omega_L t} \\ & + \sum_{j=1,2} g_s (b_j^\dagger + b_j) a_c^\dagger a_c \\ & + \frac{1}{2} \sum_{j=1,2} g_{\rm DCE} (b_j^\dagger + b_j)\big(a_c^{\dagger 2} + a_c^2\big), \end{aligned} \tag{2}$$

where $a_c^\dagger$ (a_c) and $b_j^\dagger$ (b_j) are the creation (annihilation) operators of the cavity mode and the mechanical oscillator with frequencies ω_c and ω_j, respectively. The cavity is driven weakly by a monochromatic field with frequency ω_L and strength E, which has been realized experimentally in a similar setup [42]. The second and third lines in Eq. (2) are produced by the radiation pressure, which depends quadratically on the cavity field [43,44], such that the standard SPOC (second line) and the DCE (third line) appear. Physically, the motion of the mirrors ($b_j^\dagger + b_j$) changes the cavity occupancy number ($a_c^\dagger a_c$) and produces photon pairs ($a_c^{\dagger 2} + a_c^2$). g_s and $g_{\rm DCE}$ represent the corresponding optomechanical-coupling strengths, which are determined by the zero-point-fluctuation amplitude of the mirrors, the frequency of the cavity, and the distance between two mirrors [22,43–45]. Note that $g_s = g_{\rm DCE}$ in practical optomechanical systems [22,37,43,44], and the two symbols in our case are just to distinguish the SPOC and the DCE. The time dependence of H_s can be eliminated by a rotating-frame transformation with respect to the control field frequency ω_L by introducing a unitary operator $\mathcal{O}(t) = e^{-i\omega_L a_c^\dagger a_c t}$, such that H_s can be transformed into a time-independent form via the relationship $\mathcal{H}_s = \mathcal{O}^\dagger(t) H_s \mathcal{O}(t) - i\mathcal{O}^\dagger(t)\frac{\partial \mathcal{O}(t)}{\partial t} = \mathcal{O}^\dagger(t)(H_s - \omega_L a_c^\dagger a_c)\mathcal{O}(t)$. Consequently, the effective Hamiltonian of the optomechanical system can be obtained as

$$\begin{aligned} \mathcal{H}_s = {} & \Delta_c a_c^\dagger a_c + \sum_{j=1,2} \omega_j b_j^\dagger b_j + E a_c^\dagger + E^* a_c \\ & + \sum_{j=1,2} g_s (b_j^\dagger + b_j) a_c^\dagger a_c \\ & + \frac{1}{2} \sum_{j=1,2} g_{\rm DCE} (b_j^\dagger + b_j)\big(a_c^{\dagger 2} + a_c^2\big), \end{aligned} \tag{3}$$

where $\Delta_c = \omega_c - \omega_L$ is the detuning of the cavity mode from the driving field.

The three baths are assumed to be independent of each other and take the form

$$H_b = \sum_{k\in L} \omega_{Lk} b_{Lk}^\dagger b_{Lk} + \sum_{k\in R} \omega_{Rk} b_{Rk}^\dagger b_{Rk} + \sum_{k\in C} \omega_{Ck} b_{Ck}^\dagger b_{Ck}, \tag{4}$$

where $b_{\alpha k}^\dagger$ ($b_{\alpha k}$) is the creation (annihilation) operator of a phonon or photon with state k in bath $\alpha = L, R, C$ with frequency $\omega_{\alpha k}$.

The system-bath coupling Hamiltonian is

$$\begin{aligned} H_{s-b} = {} & \sum_{k\in L} (t_{Lk,1} b_{Lk}^\dagger b_1 + t_{Lk,1}^* b_1^\dagger b_{Lk}) \\ & + \sum_{k\in R} (t_{Rk,2} b_{Rk}^\dagger b_2 + t_{Rk,2}^* b_2^\dagger b_{Rk}) \\ & + \sum_{k\in C} (t_{Ck,c} b_{Ck}^\dagger a_c + t_{Ck,c}^* a_c^\dagger b_{Ck}), \end{aligned} \tag{5}$$

where $t_{Lk,1}$ and $t_{Rk,2}$ are the coupling constants for phonon and energy transfer between the mechanical modes and the baths. $t_{Ck,c}$ is the cavity-bath coupling rate.

To study the thermal transport properties of the considered model, we employ the master-equation approach in the quantum regime. Under the framework of the Born-Markov approximation, the dynamics of the optomechanical system can be described by the following master equation [46–49]:

$$\begin{aligned} \dot\rho(t) = {} & -i[\mathcal{H}_s, \rho(t)] + \sum_{j=1,2} \sum_{\alpha=L,R} \frac{\gamma_j}{2} \{ n_B^\alpha \mathcal{L}_{b_j^\dagger}[\rho(t)] \\ & + (n_B^\alpha + 1)\mathcal{L}_{b_j}[\rho(t)]\} \\ & + \frac{\kappa_c}{2} \big\{ n_B^C \mathcal{L}_{a_c^\dagger}[\rho(t)] + \big(n_B^C + 1\big)\mathcal{L}_{a_c}[\rho(t)]\big\}, \end{aligned} \tag{6}$$

where $\rho(t)$ is the density matrix of the system. $\mathcal{L}_A[\rho(t)]$ describes the system-bath interaction for $\mathcal{L}_A[\rho(t)] = 2A\rho(t)A^\dagger - A^\dagger A\rho(t) - \rho(t)A^\dagger A$, with the operator $A = b_j^\dagger, b_j (a_c^\dagger, a_c)$ and the coupling rate $\gamma_j(\kappa_c)$ for the mechanical mode (cavity). In the wide-band limit, the coupling rates $\gamma_1(\omega) = 2\pi \sum_{k\in L} |t_{Lk,1}|^2 \delta(\omega - \omega_{Lk})$, $\gamma_2(\omega) = 2\pi \sum_{k\in R} |t_{Rk,2}|^2 \delta(\omega - \omega_{Rk})$, and $\kappa_c(\omega) = 2\pi \sum_{k\in C} |t_{Ck,c}|^2 \delta(\omega - \omega_{Ck})$ are assumed to be frequency independent. Then, we take $\gamma_j(\omega) = \gamma_j$ and $\kappa_c(\omega) = \kappa_c$.

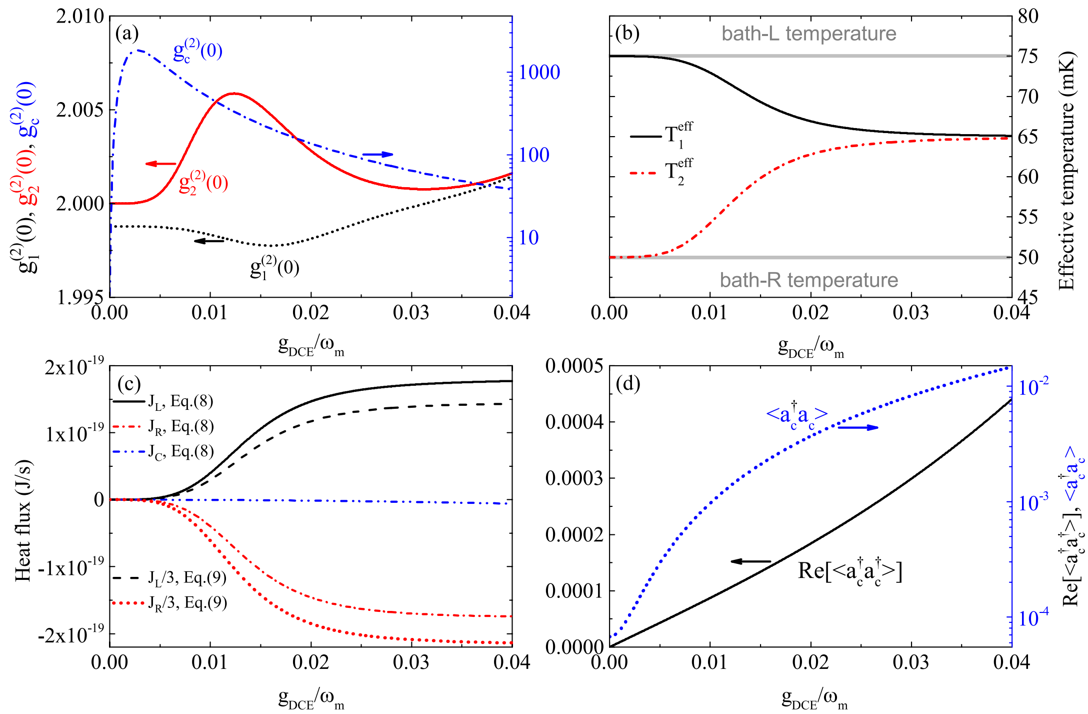

FIG. 2. (a) Equal-time second-order correlation functions $g_1^{(2)}(0)$, $g_2^{(2)}(0)$, and $g_c^{(2)}(0)$ as a function of the Casimir interaction $g_{\rm DCE}$. (b) Effective temperature of the mechanical modes $T_1^{\rm eff}$ and $T_2^{\rm eff}$ versus the Casimir interaction $g_{\rm DCE}$. (c) Heat fluxes J_L, J_R, and J_C versus the Casimir interaction $g_{\rm DCE}$ calculated by Eqs. (8) and (9). (d) Cavity mean photon number $\langle a_c^\dagger a_c\rangle$ and correlation function Re$[\langle a_c^\dagger a_c^\dagger\rangle]$ versus the Casimir interaction $g_{\rm DCE}$. The temperatures of the three baths are taken as $T_L = T_0 + \delta T$, $T_R = T_0$, and $T_C = T_0$. The other parameters are $\omega_1/2\pi = \omega_2/2\pi = \omega_m/2\pi = 5$ GHz, $\omega_c = 2\,\omega_m$, $g_s = 0.04\,\omega_m$, $\kappa_c = 10^{-6}\,\omega_m$, $\gamma_1 = 10^{-4}\,\omega_m$, $\gamma_2 = 10^{-4}\,\omega_m$, $T_0 = 50$ mK, $\delta T = 25$ mK, $\omega_L = 0$, and $E = 0$.

$n_B^\alpha = 1/(e^{\hbar\omega_j/k_BT_\alpha} - 1)$ and $n_B^C = 1/(e^{\hbar\omega_c/k_BT_C} - 1)$ are Bose-Einstein distributions, where $j = 1(2)$ corresponds to $\alpha = L(R)$. Here, we use the quantum master equation of the Lindblad form, where the system-bath interaction is assumed to be weak [50,51], that is, $\gamma_j, \kappa_c \ll \omega_j, \omega_c$. We also assume that the baths couple locally with the cavity and the mirrors, which is usually called the local master equation [52–55]. Our choice is reliable when the cavity-mirror coupling is sufficiently weak, that is, $g_s, g_{\rm DCE} \ll \omega_j, \omega_c$. Beyond this regime, one should use the global master equation, where the baths couple to global degrees of freedom of the optomechanical system [53,54,56]. If not, the violation of the second law of thermodynamics from the local master equation may take place [57,58].

The internal energy of the present system can be written as $U = \mathrm{Tr}\{\rho(t)\mathcal{H}_s\}$; then we have $\dot{U} = \mathrm{Tr}\{\dot\rho(t)\mathcal{H}_s\} + \mathrm{Tr}\{\rho(t)\dot{\mathcal{H}}_s\}$, where the first term corresponds to the total heat flux $J_{\rm tot}(t) = \mathrm{Tr}\{\dot\rho(t)\mathcal{H}_s\}$ from the baths to the system and the second term describes the power $\dot{W} = \mathrm{Tr}\{\rho(t)\dot{\mathcal{H}}_s\}$. In our case, $\dot{W} = 0$, such that $J_{\rm tot}(t) = \dot{U} = \mathrm{Tr}\{\dot\rho(t)\mathcal{H}_s\}$. Based on the master equation in Eq. (6), we have

$$
\begin{aligned}
J_{\rm tot}(t) = &\sum_{j=1,2}\sum_{\alpha=L,R}\frac{\gamma_j}{2}\mathrm{Tr}(\{n_B^\alpha\mathcal{L}_{b_j^\dagger}[\rho(t)] \\
&+ (n_B^\alpha + 1)\mathcal{L}_{b_j}[\rho(t)]\}\mathcal{H}_s) \\
&+ \frac{\kappa_c}{2}\mathrm{Tr}\big(\big\{n_B^C\mathcal{L}_{a_c^\dagger}[\rho(t)] + \big(n_B^C + 1\big)\mathcal{L}_{a_c}[\rho(t)]\big\}\mathcal{H}_s\big).
\end{aligned} \tag{7}
$$

Finally, the heat flux flowing from the baths to the system can be defined as

$$
J_\alpha(t) = \frac{\chi}{2}\mathrm{Tr}(\{n_B^\alpha\mathcal{L}_{\beta^\dagger}[\rho(t)] + (n_B^\alpha + 1)\mathcal{L}_\beta[\rho(t)]\}\mathcal{H}_s), \tag{8}
$$

where α labels the bath and its annihilation operator is marked by β. χ is the coupling strength between the bosonic mode and the bath. Here, $\alpha = L, R, C$ corresponds to $\beta = b_1, b_2, a_c$ and $\chi = \gamma_1, \gamma_2, \kappa_c$. In the steady state, $\dot{U} = \mathrm{Tr}\{\dot\rho(\infty)\mathcal{H}_s\} = 0$, one can get the energy conservation, that is, $J_L + J_R + J_C = 0$ for $t \to \infty$. To calculate the heat flux $J_{L,R,C}$, one needs to get the steady-state density matrix. The matrix elements of the cavity-mirror density operator $\rho(t)$ can be defined as $\rho_{n_c,n_1,n_2;n_c',n_1',n_2'}(t) := \langle n_c, n_1, n_2|\rho(t)|n_c', n_1', n_2'\rangle$, where $n_c(n_c')$ and $n_1, n_2(n_1', n_2')$ refer to the Fock states of the cavity and the mechanical modes. By using Eq. (6), we can obtain the time evolution of the matrix elements, such as $\dot\rho_{n_c,n_1,n_2;n_c',n_1',n_2'}(t)$. In the steady state, $\dot\rho_{n_c,n_1,n_2;n_c',n_1',n_2'}(\infty) = 0$, a coupled set of equations can be found. By truncating the bosonic Hilbert space in a certain order, for our case $\max\{n_c, n_1, n_2, n_c', n_1', n_2'\} = 5$, the steady-state matrix elements can be achieved.

On the other hand, one may use the empirical formula to calculate the steady-state flux [27,42]

$$
J_\alpha = \chi k_B\big(T_\alpha - T_{\mathcal{B}}^{\rm eff}\big), \tag{9}
$$

where $\alpha = L, R, C$ corresponds to $\mathcal{B} = 1, 2, c$ and $\chi = \gamma_1, \gamma_2, \kappa_c$. $T_{1,2,c}^{\rm eff}$ represents the effective temperature of the mechanical modes and the cavity mode. When the three bosonic modes are in the thermal state [59], we can define their

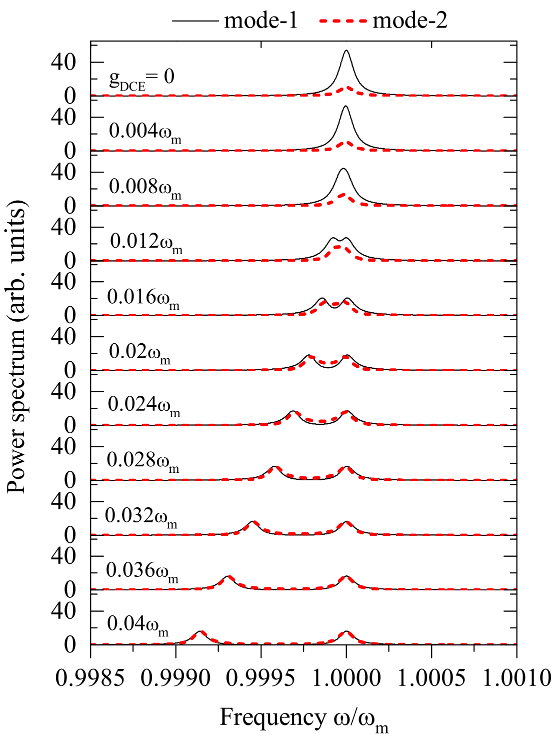

FIG. 3. Frequency dependence of the mechanical power spectrum $\mathcal{S}_1(\omega)$ (black solid line) and $\mathcal{S}_2(\omega)$ (red dashed line) calculated for different $g_{\rm DCE}$. The other parameters are the same as in Fig. 2.

effective temperatures as

$$T^{\rm eff}_{1,2,c} = \frac{\hbar\omega_{1,2,c}/k_B}{\ln(1/\langle n_{1,2,c}\rangle + 1)}, \tag{10}$$

where $n_j = b_j^\dagger b_j$ and $n_c = a_c^\dagger a_c$. Note that the effective temperature is defined under the assumption that the bosonic modes are in thermal equilibrium. In general, the equal-time second-order correlation functions can be used to characterize the states of the three bosonic modes and test the applicability of the effective temperature and are defined as

$$g_j^{(2)}(0) = \frac{\langle b_j^\dagger b_j^\dagger b_j b_j\rangle}{\langle b_j^\dagger b_j\rangle^2}, \quad g_c^{(2)}(0) = \frac{\langle a_c^\dagger a_c^\dagger a_c a_c\rangle}{\langle a_c^\dagger a_c\rangle^2}. \tag{11}$$

III. RESULTS AND DISCUSSION

Before showing the results, we note that both the SPOC and the DCE exist in real optomechanical systems [22,27,37,42–44]. For $\omega_j \ll \omega_c$, the DCE can be ignored [2]. For $\omega_j \sim \omega_c$, both the SPOC and the DCE may play a key role in the heat transfer. In Figs. 2–4, and 9. we will fix g_s ($g_{\rm DCE}$) to study the dependence of heat transfer on the DCE (SPOC).

A. DCE-induced heat transfer

First, we consider that the cavity is not driven by coherent light, that is, $\omega_L = 0$ and $E = 0$. In Fig. 2(a) the equal-time second-order correlation functions for the cavity $g_c^{(2)}(0)$ and the mechanical mode $g_j^{(2)}(0)$ are calculated as a function of the Casimir interaction $g_{\rm DCE}$. For $g_{\rm DCE} = 0$, the three bosonic

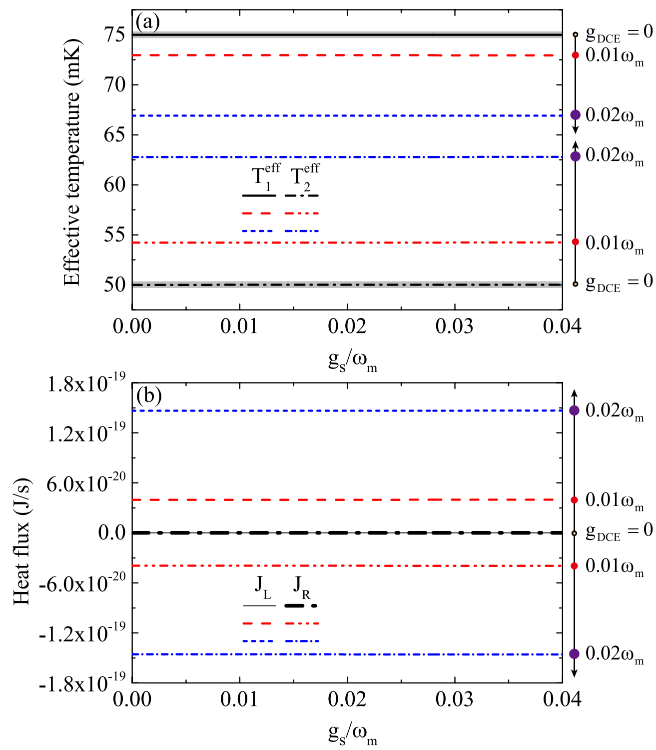

FIG. 4. (a) Effective temperature of the mechanical modes $T_1^{\rm eff}$ and $T_2^{\rm eff}$ as a function of the SPOC g_s for the indicated values of the Casimir interaction $g_{\rm DCE}$. The temperature of bath L (R) is marked by upper (lower) shading. (b) Similar to (a), but for heat fluxes J_L and J_R. The other parameters are the same as in Fig. 2.

modes are respectively coupled to a thermal bath and therefore in the thermal state, such that $g_c^{(2)}(0) \approx 2$, $g_1^{(2)}(0) \approx 2$, and $g_2^{(2)}(0) \approx 2$. When $g_{\rm DCE}$ increases, $g_c^{(2)}(0)$ is always greater than 2, indicating that the Casimir photon pair is emitted from the cavity. Meanwhile, the two mechanical modes are in the thermal state even for large values of $g_{\rm DCE}$. Then, we can introduce an effective temperature $T_j^{\rm eff}$ to describe the thermodynamic properties of the mechanical mode j, as shown in Fig. 2(b). When $g_{\rm DCE} = 0$, the two mechanical modes have the same temperature as the baths near them, that is, $T_1^{\rm eff} = T_L$ and $T_2^{\rm eff} = T_R$. As expected, $T_1^{\rm eff}$ ($T_2^{\rm eff}$) decreases (increases) with increasing $g_{\rm DCE}$, and finally, the two mechanical modes have almost the same temperature, with $T_1^{\rm eff} \approx T_2^{\rm eff}$. The reason is as follows. Both mechanical modes are coupled to the cavity; then a nonlocal interaction between the mechanical modes is established through the DCE. Therefore, the mechanical quantum excitations and energies can be exchanged between them. As a result, a net heat flux can be produced, as shown in Fig. 2(c). We consider two approaches, indicated by Eqs. (8) and (9), to calculate the heat flux. The heat flux flowing from the baths (L and R) to the system for the two methods are consistent qualitatively. Note that the energy conservation from Eq. (8) is satisfied, that is, $J_L + J_R + J_C = 0$. We cannot define an effective temperature for the cavity mode in the bunched state, so the heat flux from the corresponding bath to the system is not calculated by Eq. (9).

It is noted that the results in Figs. 2(a)–2(c) are obtained by setting $g_s = 0.04\omega_m$. Even in the presence of the SPOC, the cavity and the mechanical modes do not deviate from their thermal equilibrium with the baths when the DCE is absent. Consequently, we attribute the observed energy transfer solely to the indirect mechanical coupling induced by the DCE, which is consistent with a recent experiment [27]. The behavior is also visible in the DCE dependence of the cavity mean photon number $\langle a_c^\dagger a_c \rangle$ and correlation function $\mathrm{Re}[\langle a_c^\dagger a_c^\dagger \rangle]$ [see Fig. 2(d)]. As g_{DCE} increases from 0 to $0.04\,\omega_m$, the value of $\langle a_c^\dagger a_c \rangle$ does not start from 0 because the cavity is coupled to a nonzero temperature bath. The finite populations in the cavity cannot lead to an energy exchange between the two mechanical modes, as shown in Figs. 2(b) and 2(c). However, a finite value of g_{DCE} yields a correlation of $\mathrm{Re}[\langle a_c^\dagger a_c^\dagger \rangle] = \mathrm{Re}[\langle a_c a_c \rangle]$, which can build a nonlocal interaction between the mechanical modes induced by the Casimir two-photon process.

The power spectrum for the two mechanical modes, $\mathcal{S}_j(\omega) = \int_{-\infty}^{\infty} \langle b_j^\dagger(t) b_j(0) \rangle e^{-i\omega t} dt$, is shown in Fig. 3 for different g_{DCE}. When the DCE is weak, the mechanical spectrum exhibits one peak for each mode, although the heights of the two peaks are different due to the temperature bias applied. This indicates that the two mechanical modes are not coupled via the DCE. For large g_{DCE}, mechanical spectra with two well-defined peaks are displayed, where the mode splitting occurs, and the separation between the peaks increases by increasing g_{DCE}. Thus, we claim that an effective exchange interaction between the mechanical modes becomes enhanced with increasing g_{DCE}. Such a dependence is consistent with Figs. 2(b) and 2(c), as observed in a recent experiment [27].

In order to further reveal how the DCE influences the heat transfer, Fig. 4(a) shows the variation of T_1^{eff} and T_2^{eff} with g_s for indicated values of g_{DCE}. In the absence of the DCE, that is, $g_{\mathrm{DCE}} = 0$, one can see that $T_1^{\mathrm{eff}} = T_L$ and $T_2^{\mathrm{eff}} = T_R$. Thus, the heat transfer becomes suppressed and disappears completely; see the black solid (dashed) line ($J_L = J_R = 0$) in Fig. 4(b). Once the DCE is introduced, the effective temperature of mechanical mode 1 (2) is always less (larger) than the temperature of bath L (R), that is, $T_1^{\mathrm{eff}} < T_L$ and $T_2^{\mathrm{eff}} > T_R$, indicating that the modes deviate from thermal equilibrium with the baths. Consequently, the heat flux becomes nonzero, and its value depends on the relative magnitude of the Casimir interaction; that is, J_L and $-J_R$ increase by increasing g_{DCE}. Note that the values of $T_{1,2}^{\mathrm{eff}}$ and $J_{L,R}$ are almost unchanged by varying g_s. Thus, the key implication from the above discussion is that the energy transfer between the mechanical modes is caused by only the DCE. This again directly proves the results in Fig. 2.

B. Resonance-enhanced heat transfer

The heat transfer discussed above is determined by the strength of the DCE. If the DCE is very weak, such as $g_{\mathrm{DCE}} < 0.004\,\omega_m$, mechanical mode 1 decouples completely from mechanical mode 2, and the heat transport vanishes [see Figs. 2(b), 2(c) and 3]. Figure 5(a) displays the heat flux $J_{L,R,C}$ versus the cavity frequency ω_c. As $\omega_c < 0.5\,\omega_m$ ($\omega_c > 0.5\,\omega_m$) increases (decreases) approaching the resonant position $\omega_c = 0.5\,\omega_m$, the heat transfer is enhanced substantially. This is because the energy conversion of the cavity to the mechanical modes induced by the resonant DCE is energetically

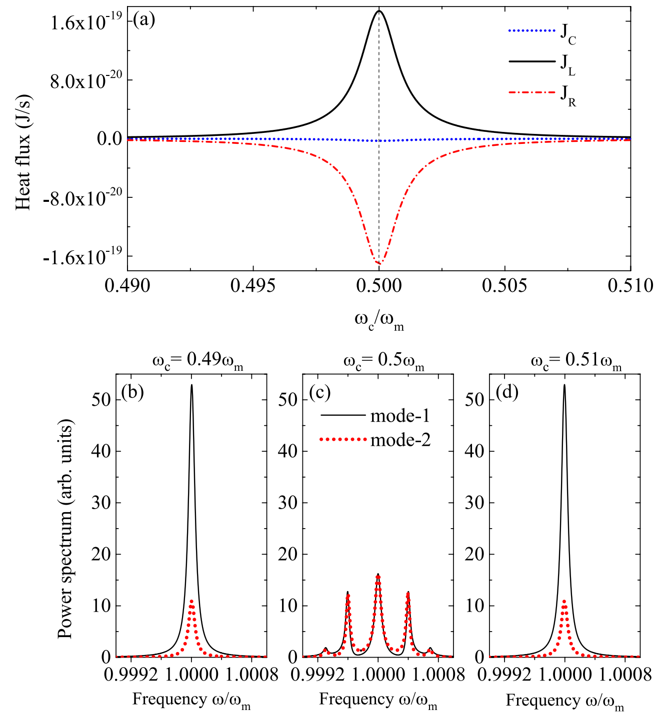

FIG. 5. (a) Heat fluxes J_L, J_R, and J_C as a function of the cavity frequency ω_c. Frequency dependence of the power spectrum calculated for (b) $\omega_c = 0.49\,\omega_m$, (c) $\omega_c = 0.5\,\omega_m$, and (d) $\omega_c = 0.51\,\omega_m$. Both the SPOC and the DCE are considered here, and we take $g_s = g_{\mathrm{DCE}} = 0.0004\,\omega_m$. The other parameters are the same as in Fig. 2.

favorable to achieve the resonance-enhanced heat transfer between the mechanical modes. Correspondingly, mechanical mode splitting at the resonant frequency is clearly shown in the power spectrum [see Fig. 5(c)]. When the cavity frequency deviates from the resonance, the mechanical mode splitting disappears [see Figs. 5(b) and 5(d)], and consequently, the heat fluxes J_L and $-J_R$ decrease significantly. Unlike the case in Fig. 2, the resonance-enhanced heat transfer does not rely on the large g_{DCE}, indicating that the energy transfer between mirrors may take place when they are far apart, for example, in the range of a few hundred nanometers. In this region, the energy transfer induced by the near-field thermal radiation almost disappears [60–66]. Meanwhile, the near-field thermal radiation is independent of the frequency matching. In such a case, the role of the DCE in energy transfer may be highlighted. Our proposal was not observed experimentally [27] and is a consequence of a resonance-enhanced energy transfer process. We note that, in many optomechanics experiments, the mechanical frequency of the mirror is far from the cavity frequency. To make the cavity and mechanical modes resonate, one can tune the cavity frequency by squeezing itself [34,67–69].

Figure 6(a) presents the heat flux $J_{L,R}$ as a function of the optomechanical-coupling strength $g_s = g_{\mathrm{DCE}}$ for different values of the cavity frequency ω_c. When the cavity frequencies are comparable to the mechanical frequency, $0.49\,\omega_m \leqslant \omega_c \leqslant 2\,\omega_m$, the heat fluxes are independent of ω_c for large $g_s = g_{\mathrm{DCE}}$. However, at high cavity frequencies $\omega_c \gg \omega_m$, J_L and $-J_R$ decrease with increasing ω_c for the whole range of

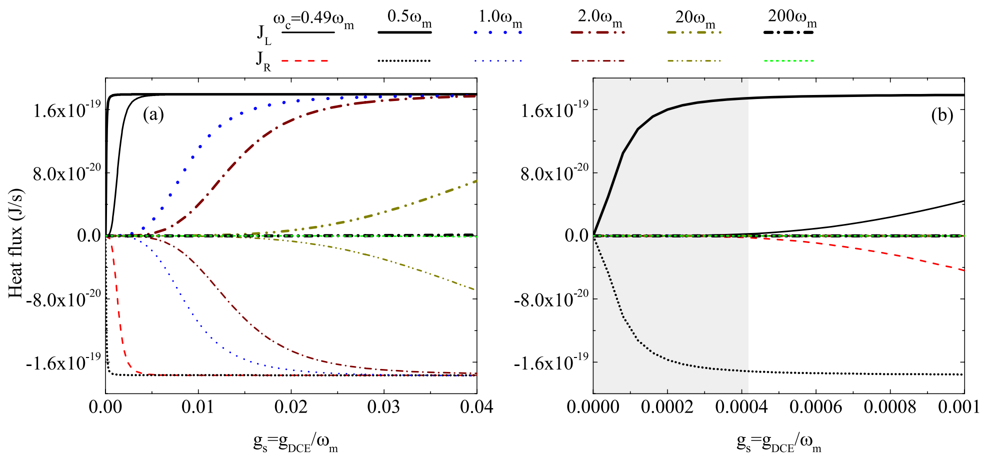

FIG. 6. (a) Heat fluxes J_L and J_R as a function of the optomechanical-coupling strength $g_s = g_{\rm DCE}$ for different cavity frequencies ω_c. (b) Enlarged image of the region $(0, 0.001\,\omega_m)$ in (a). The other parameters are the same as in Fig. 5.

$g_s = g_{\rm DCE}$. In this case, for example, $\omega_c = 200\,\omega_m$, the role of the DCE in the heat transfer can almost be ignored. Here, we focus on the weak-optomechanical-coupling case, as shown in Fig. 6(b). As expected, the resonant DCE for $\omega_c = 0.5\,\omega_m$ results in an effective mechanical coupling, and hence, the heat transfer is enhanced significantly, which is more pronounced in the shading marked in Fig. 6(b). We show the case of weak cavity-bath coupling in Fig. 5. By increasing the coupling rate κ_c, an activated behavior of the heat flux is not found in Fig. 7. This means that the resonance-enhanced heat transfer weakly relies on κ_c. Note that, for $\kappa_c = 0$, our device is simplified to the two-terminal case, such that $J_L = -J_R$.

In Fig. 8, we plot the heat flux $J_{L,R,C}$ as a function of the mechanical frequency ω_2 for $\omega_1 = \omega_m$ and $\omega_c = 0.5\,\omega_m$. At $\omega_2 = \omega_1$, the cavity and the mechanical modes are resonant, resulting in an enhanced heat transfer between the mechanical modes, as discussed in Fig. 5. It is obvious that for $\omega_2 \neq \omega_1$, the efficiency of the energy transfer is significantly reduced. As shown in the inset, in the nonresonant region $\omega_2 \in (0.993\,\omega_1, 0.995\,\omega_1)$, the heat flux injected from the left bath mainly flows into the bath coupled to the cavity instead of the right one. Thus, the energy exchange between the mechanical modes cannot be established effectively. This indicates that the resonance-enhanced energy transfer in Fig. 5 is more pronounced when the mechanical frequencies ω_1 and ω_2 are closer to each other.

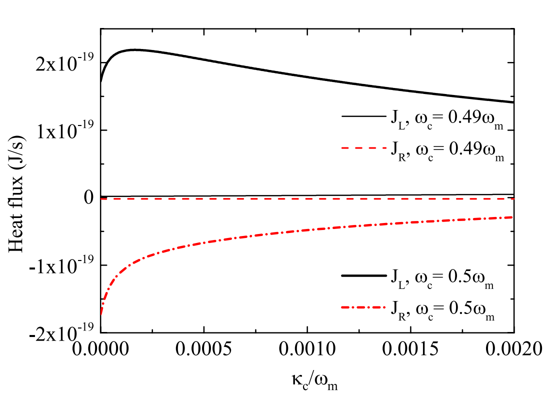

FIG. 7. Heat fluxes J_L and J_R as a function of the cavity-bath coupling rate κ_c for two cavity frequencies, $\omega_c = 0.49\,\omega_m$ and $\omega_c = 0.5\,\omega_m$. The other parameters are the same as in Fig. 5.

C. Laser-driven cavity

In Secs. III A and III B, the heat transfer is dominated by the DCE when the cavity is not driven by coherent light. Once the laser is introduced, the SPOC-induced indirect interaction between mechanical modes can be observed, such that the heat flux can be driven by a temperature bias [41,42], where the DCE is not considered. Thus, it is also interesting to study the DCE-dependent heat flux in the presence of the coherent light, as shown in Fig. 9. The contribution of the SPOC to heat transfer is mainly due to cavity-induced nonlocal interactions, as discussed in previous studies [41,42]. The explicit DCE dependence of the heat flux may provide important information about such optomechanical systems. Especially, the DCE-mediated heat transfer survives even for $\omega_c \gg \omega_m$ (not shown here). This indicates that both the SPOC and the DCE can yield nonlocal energy transfer, which can be

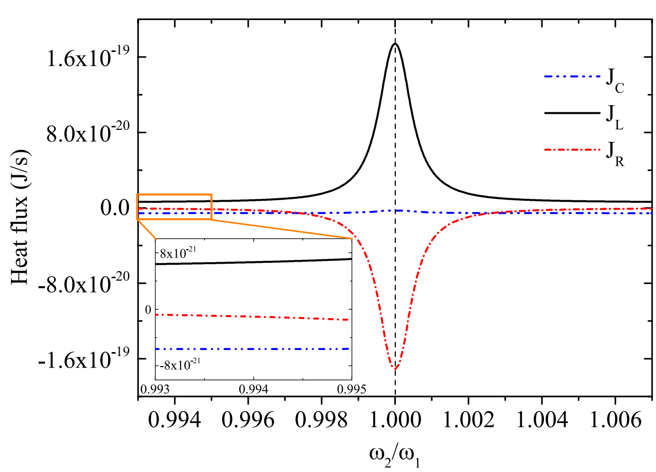

FIG. 8. Heat fluxes J_L, J_R, and J_C as a function of the mechanical frequency ω_2 with $\omega_1 = \omega_m$ and $\omega_c = 0.5\,\omega_m$. The inset shows an enlarged image of the region $(0.993\,\omega_2/\omega_1, 0.995\,\omega_2/\omega_1)$. The other parameters are the same as in Fig. 5.

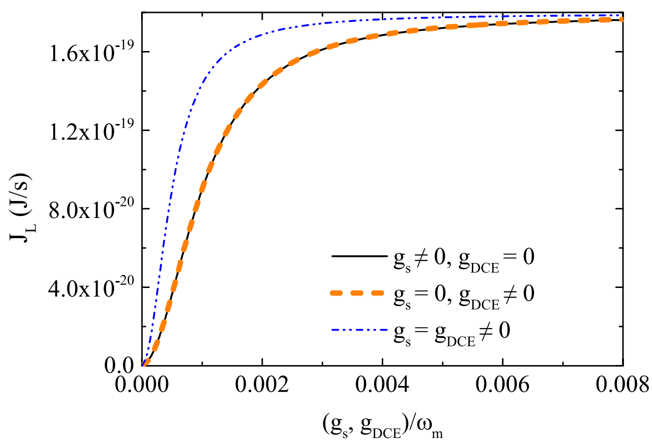

FIG. 9. Heat flux J_L as a function of the optomechanical-coupling strength (g_s, $g_{\rm DCE}$). For the laser, we take $\omega_L = \omega_c - \omega_m$ and $E = 0.05\,\omega_m$. The other parameters are the same as in Fig. 2.

further enhanced by combining the two interactions. In this case, one cannot separate out the role of the DCE in heat transfer from the optomechanical couplings.

Let us now study how the laser field affects the energy transfer process. We plot the dependence of the heat flux $J_{L,R}$ on the laser frequency ω_L in Fig. 10(a). It is clear that local maxima of J_L and $-J_R$ appear at the point where $\omega_L = 1.5\,\omega_m$ (equivalent to $\Delta_c = 0.5\,\omega_m$), which can be attributed to the resonance-enhanced energy transfer. In this case, both the SPOC and the DCE are considered, while the resonance-enhanced heat transfer is induced by the DCE. This is because $g_c^{(2)}(0)$ is greater than 2 in the resonant regime [see Fig. 10(b)], indicating that the bunched photons induced by the DCE emitted from the cavity appear. As expected, a maximum value of $\langle a_c^\dagger a_c\rangle$ is also obtained around the resonant point, as shown in Fig. 10(b). Thus, the heat transfer induced by the DCE in such optomechanical systems can then be controlled by a laser field and can be completely enhanced by resonance. In detail, energy can be transferred from one mechanical mode to the other in a controlled way. This is thanks to the controlled modulation of the laser frequency ω_L, which can make the cavity and mechanical modes reach resonance. Very recently, laser-controlled heat transfer mediated by the SPOC was realized experimentally [42]; one may expect its application to the resonance-enhanced process manifested by the DCE.

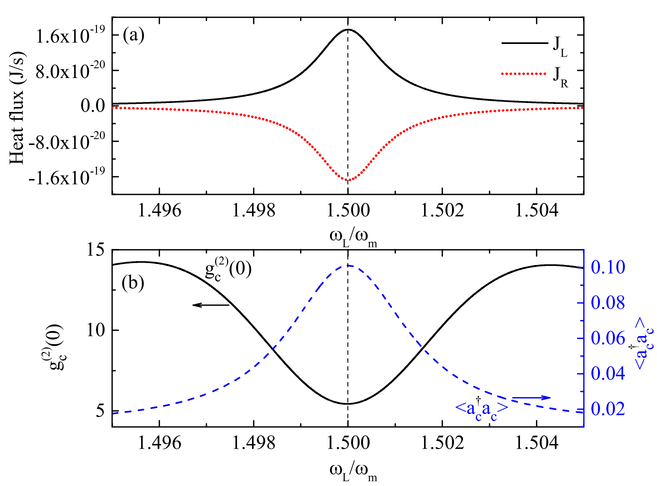

FIG. 10. Laser field dependence of heat fluxes J_L and J_R for $g_s = g_{\rm DCE} = 0.0004\,\omega_m$. (b) The same as in (a) calculated for the cavity equal-time second-order correlation function $g_c^{(2)}(0)$ and mean photon number $\langle a_c^\dagger a_c\rangle$. The other parameters are the same as in Fig. 9.

IV. CONCLUSION AND OUTLOOK

By employing the quantum master-equation method, we studied the effect of the SPOC and the DCE on the heat transfer in an optomechanical system composed of one optical cavity and two mechanical resonators with or without a laser field. In the absence of the laser, we remark that only the DCE-induced indirect coupling between mechanical modes can yield an observable heat transfer driven by a temperature bias, which is consistent with a recent experiment [27]. When the cavity is driven by the laser, the nonlocal heat transfer induced by both the SPOC and the DCE can be found. Particularly interesting for applications is our finding of the resonant-DCE-enhanced heat transfer. This not only provides a possibility to control the energy transfer actively but also allows one to highlight its dependence on the DCE.

In our model, the cavity contains only one mode, which is a valid approximation when the other cavity modes cannot be excited effectively by the mechanical motion of the mirrors. This happens when the frequencies of the cavity modes are not evenly distributed in space [70,71] or the mechanical frequencies are far from the frequency spacing between neighboring cavity modes [43,44,72,73]. Beyond this approximation, an important consequence of the introduction of a multimode cavity with mode-mode coupling is that extra transport channels between mechanical modes appear. Then, the heat transfer induced by the DCE in the resonant region may be enhanced, which remains to be analyzed.

Another platform that achieves the DCE is superconducting circuits [32,74], where a superconducting quantum interference device (SQUID) is positioned near the transmission line and then the boundary condition of the line can be adjusted by the SQUID. Recently, a doubly tunable superconducting resonator has been proposed to produce a microwave photon induced by the DCE [75], in which both ends are coupled to a SQUID. When the two SQUIDs are pumped by magnetic fluxes with different phases, the device is equivalent to a cavity with two movable mirrors; then the generation of photons by the resonant DCE is affected by the interference effects. From the perspective of heat transport, how one captures the interference effects in thermodynamic signals (such as heat flux) induced by the DCE is interesting. In turn, it is also possible to use such interference effects to regulate heat transport.

ACKNOWLEDGMENTS

This work is supported by the National Natural Science Foundation of China (Grant No. 21873033), the China Postdoctoral Science Foundation (Grant No. 2020M672322), the National Key Research and Development Program of China (Grant No. 2017YFA0403501), and the program for the HUST academic frontier youth team.

[1] P. Meystre, Ann. Phys. (Berlin, Ger.) **525**, 215 (2013).
[2] M. Aspelmeyer, T. J. Kippenberg, and F. Marquardt, Rev. Mod. Phys. **86**, 1391 (2014).
[3] M. Aspelmeyer, T. J. Kippenberg, and F. Marquardt, *Cavity Optomechanics: Nano- and Micromechanical Resonators Interacting with Light* (Springer, Heidelberg, 2014).
[4] M. Metcalfe, Appl. Phys. Rev. **1**, 031105 (2014).
[5] P. Rabl, Phys. Rev. Lett. **107**, 063601 (2011).
[6] J.-Q. Liao and F. Nori, Phys. Rev. A **88**, 023853 (2013).
[7] X.-W. Xu and Y.-J. Li, J. Phys. B **46**, 035502 (2013).
[8] B. Sarma and A. K. Sarma, Phys. Rev. A **98**, 013826 (2018).
[9] W. Marshall, C. Simon, R. Penrose, and D. Bouwmeester, Phys. Rev. Lett. **91**, 130401 (2003).
[10] O. Arcizet, P.-F. Cohadon, T. Briant, M. Pinard, and A. Heidmann, Nature (London) **444**, 71 (2006).
[11] D. Kleckner and D. Bouwmeester, Nature (London) **444**, 75 (2006).
[12] S. Gigan, H. Böhm, M. Paternostro, F. Blaser, G. Langer, J. Hertzberg, K. C. Schwab, D. Bäuerle, M. Aspelmeyer, and A. Zeilinger, Nature (London) **444**, 67 (2006).
[13] A. Schliesser, P. Del'Haye, N. Nooshi, K. J. Vahala, and T. J. Kippenberg, Phys. Rev. Lett. **97**, 243905 (2006).
[14] A. A. Clerk, F. Marquardt, and K. Jacobs, New J. Phys. **10**, 095010 (2008).
[15] T. Rocheleau, T. Ndukum, C. Macklin, J. Hertzberg, A. Clerk, and K. Schwab, Nature (London) **463**, 72 (2010).
[16] J. D. Teufel, T. Donner, D. Li, J. W. Harlow, M. Allman, K. Cicak, A. J. Sirois, J. D. Whittaker, K. W. Lehnert, and R. W. Simmonds, Nature (London) **475**, 359 (2011).
[17] S. Bose, K. Jacobs, and P. L. Knight, Phys. Rev. A **56**, 4175 (1997).
[18] S. Mancini, V. I. Man'ko, and P. Tombesi, Phys. Rev. A **55**, 3042 (1997).
[19] H. Xu, D. Mason, L. Jiang, and J. Harris, Nature (London) **537**, 80 (2016).
[20] M. J. Weaver, F. Buters, F. Luna, H. Eerkens, K. Heeck, S. d. Man, and D. Bouwmeester, Nat. Commun. **8**, 824 (2017).
[21] R. Riedinger, A. Wallucks, I. Marinković, C. Löschnauer, M. Aspelmeyer, S. Hong, and S. Gröblacher, Nature (London) **556**, 473 (2018).
[22] O. Di Stefano, A. Settineri, V. Macrì, A. Ridolfo, R. Stassi, A. F. Kockum, S. Savasta, and F. Nori, Phys. Rev. Lett. **122**, 030402 (2019).
[23] C. Ockeloen-Korppi, E. Damskägg, J.-M. Pirkkalainen, M. Asjad, A. Clerk, F. Massel, M. Woolley, and M. Sillanpää, Nature (London) **556**, 478 (2018).
[24] H. Xu, L. Jiang, A. Clerk, and J. Harris, Nature (London) **568**, 65 (2019).
[25] S.-S. Chen, H. Zhang, Q. Ai, and G.-J. Yang, Phys. Rev. A **100**, 052306 (2019).
[26] J. P. Mathew, J. del Pino, and E. Verhagen, Nat. Nanotechnol. **15**, 198 (2020).
[27] K. Y. Fong, H.-K. Li, R. Zhao, S. Yang, Y. Wang, and X. Zhang, Nature (London) **576**, 243 (2019).
[28] J. Schwinger, Phys. Rev. **82**, 664 (1951).
[29] S. W. Hawking, Nature (London) **248**, 30 (1974).
[30] W. G. Unruh, Phys. Rev. D **14**, 870 (1976).
[31] G. T. Moore, J. Math. Phys. **11**, 2679 (1970).
[32] C. M. Wilson, G. Johansson, A. Pourkabirian, M. Simoen, J. R. Johansson, T. Duty, F. Nori, and P. Delsing, Nature (London) **479**, 376 (2011).
[33] V. Macrì, A. Ridolfo, O. Di Stefano, A. F. Kockum, F. Nori, and S. Savasta, Phys. Rev. X **8**, 011031 (2018).
[34] W. Qin, V. Macrì, A. Miranowicz, S. Savasta, and F. Nori, Phys. Rev. A **100**, 062501 (2019).
[35] N. F. Del Grosso, F. C. Lombardo, and P. I. Villar, Phys. Rev. A **100**, 062516 (2019).
[36] S. Butera and I. Carusotto, Phys. Rev. A **99**, 053815 (2019).
[37] A. Settineri, V. Macrì, L. Garziano, O. Di Stefano, F. Nori, and S. Savasta, Phys. Rev. A **100**, 022501 (2019).
[38] A. Xuereb, C. Genes, G. Pupillo, M. Paternostro, and A. Dantan, Phys. Rev. Lett. **112**, 133604 (2014).
[39] S. Barzanjeh, M. Aquilina, and A. Xuereb, Phys. Rev. Lett. **120**, 060601 (2018).
[40] A. Seif, W. DeGottardi, K. Esfarjani, and M. Hafezi, Nat. Commun. **9**, 1207 (2018).
[41] S. M. Ashrafi, R. Malekfar, A. R. Bahrampour, and J. Feist, Phys. Rev. A **100**, 013826 (2019).
[42] C. Yang, X. Wei, J. Sheng, and H. Wu, Nat. Commun. **11**, 4656 (2020).
[43] C. K. Law, Phys. Rev. A **49**, 433 (1994).
[44] C. K. Law, Phys. Rev. A **51**, 2537 (1995).
[45] S. Butera and R. Passante, Phys. Rev. Lett. **111**, 060403 (2013).
[46] C. W. Gardiner, *Handbook of Stochastic Methods* (Springer, Berlin, 1985), Vol. 3.
[47] M. O. Scully and M. S. Zubairy, *Quantum Optics* (Cambridge University Press, Cambridge, 1997).
[48] H.-P. Breuer and F. Petruccione, *The Theory of Open Quantum Systems* (Oxford University Press, Oxford, 2002).
[49] H. J. Carmichael, *Statistical Methods in Quantum Optics 1: Master Equations and Fokker-Planck Equations* (Springer, Berlin, 1999).
[50] G. Lindblad, Commun. Math. Phys. **48**, 119 (1976).
[51] H. Wichterich, M. J. Henrich, H.-P. Breuer, J. Gemmer, and M. Michel, Phys. Rev. E **76**, 031115 (2007).
[52] A. Purkayastha, A. Dhar, and M. Kulkarni, Phys. Rev. A **93**, 062114 (2016).
[53] P. P. Hofer, M. Perarnau-Llobet, L. D. M. Miranda, G. Haack, R. Silva, J. B. Brask, and N. Brunner, New J. Phys. **19**, 123037 (2017).
[54] J. O. González, L. A. Correa, G. Nocerino, J. P. Palao, D. Alonso, and G. Adesso, Open Syst. Inf. Dyn. **24**, 1740010 (2017).
[55] A. U. C. Hardal, N. Aslan, C. M. Wilson, and O. E. Müstecaplıoğlu, Phys. Rev. E **96**, 062120 (2017).
[56] S. Khandelwal, N. Palazzo, N. Brunner, and G. Haack, New J. Phys. **22**, 073039 (2020).
[57] B. Gardas and S. Deffner, Phys. Rev. E **92**, 042126 (2015).
[58] S. Seah, S. Nimmrichter, and V. Scarani, Phys. Rev. E **98**, 012131 (2018).
[59] T. Wang, L.-L. Nian, and J.-T. Lü, Phys. Rev. E **102**, 022127 (2020).
[60] A. Kittel, W. Müller-Hirsch, J. Parisi, S.-A. Biehs, D. Reddig, and M. Holthaus, Phys. Rev. Lett. **95**, 224301 (2005).
[61] K. Kim, B. Song, V. Fernández-Hurtado, W. Lee, W. Jeong, L. Cui, D. Thompson, J. Feist, M. T. H. Reid, F. J. García-Vidal, J. C. Cueva, E. Meyhofer, and P. Reddy, Nature (London) **528**, 387 (2015).

[62] B. Song, D. Thompson, A. Fiorino, Y. Ganjeh, P. Reddy, and E. Meyhofer, Nat. Nanotechnol. **11**, 509 (2016).

[63] L. Cui, W. Jeong, V. Fernández-Hurtado, J. Feist, F. J. García-Vidal, J. C. Cuevas, E. Meyhofer, and P. Reddy, Nat. Commun. **8**, 14479 (2017).

[64] K. Kloppstech, N. Könne, S.-A. Biehs, A. W. Rodriguez, L. Worbes, D. Hellmann, and A. Kittel, Nat. Commun. **8**, 14475 (2017).

[65] Z.-Q. Zhang, J.-T. Lü, and J.-S. Wang, Phys. Rev. B **97**, 195450 (2018).

[66] J.-S. Wang, Z.-Q. Zhang, and J.-T. Lü, Phys. Rev. E **98**, 012118 (2018).

[67] X.-Y. Lü, Y. Wu, J. R. Johansson, H. Jing, J. Zhang, and F. Nori, Phys. Rev. Lett. **114**, 093602 (2015).

[68] W. Qin, A. Miranowicz, P.-B. Li, X.-Y. Lü, J. Q. You, and F. Nori, Phys. Rev. Lett. **120**, 093601 (2018).

[69] C. Leroux, L. C. G. Govia, and A. A. Clerk, Phys. Rev. Lett. **120**, 093602 (2018).

[70] M. Crocce, D. A. R. Dalvit, and F. D. Mazzitelli, Phys. Rev. A **64**, 013808 (2001).

[71] F. C. Lombardo, F. D. Mazzitelli, A. Soba, and P. I. Villar, Phys. Rev. A **98**, 022512 (2018).

[72] A. F. Pace, M. J. Collett, and D. F. Walls, Phys. Rev. A **47**, 3173 (1993).

[73] S. Mancini and P. Tombesi, Phys. Rev. A **49**, 4055 (1994).

[74] J. R. Johansson, G. Johansson, C. M. Wilson, and F. Nori, Phys. Rev. A **82**, 052509 (2010).

[75] I.-M. Svensson, M. Pierre, M. Simoen, W. Wustmann, P. Krantz, A. Bengtsson, G. Johansson, J. Bylander, V. Shumeiko, and P. Delsing, J. Phys.: Conf. Ser. **969**, 012146 (2018).